A. Zelei, B. Krauskopf, T. Insperger: Control optimization for a three-segmented hopping leg model of human locomotion. In: 14th International Conference on Dynamical Systems Theory and Applications, December 11-14, 2017, Lodz, POLAND.

Control optimization for a three-segmented hopping leg model of human locomotion

Ambrus Zelei, Bernd Krauskopf, Tamás Insperger

Abstract: The research of human and robotic legged locomotion applies dynamic models with a wide range of complexity and aims to answer many different questions. In our research we focus on the effect of kinematic parameters and foot placement techniques on the ground-foot impact intensity. Our method is to use the multibody dynamic model of a segmented leg. We obtain a quantitative measure for the foot collision intensity by analytic calculations. The pre-impact velocity conditions are obtained by a hopping three-segmented planar leg model that imitates pedal locomotion. The single legged model contains the foot, the shank, the thigh and a reaction wheel attached in the hip. Stable periodic motion, i.e. hopping was achieved by means of control torques in the ankle, the knee and the hip joint. Different control strategies are specified for the grounded and flight phase. The parameters of the linear feedback controller are tuned to optimise different cost functions, such as running speed, energy efficiency and impact intensity. We also investigate how the stability of periodic motion depends on the control gains.

1. Introduction

Understanding of human walking, running, jumping and the development of corresponding bipedal robots require thorough analysis of complex dynamic models. Although, there are many experimental and theoretical results, analysis of bipedal locomotion of humans and mobile robots are still in the center of interests of biomechanics. In this paper, we develop a segmented leg model, which can describe stable periodic motion associated with hopping.

1.1. Motivations

A yet unresolved issue is the effect of running kinematics and foot placement pattern on the ground-foot collision intensity. Depending on the form of running, high impacts and therefore high kinetic energy absorption may occur, which should actually be avoided in order to minimize the risk of injuries and also to increase energy efficiency during running [7,9,11,14]. The hopping leg model presented in this paper provides measures for the ground-foot collision, like kinetic energy absorption and effective mass. The model provides realistic pre-impact configuration.

In spite of the large number of publications, the mechanism of human balancing is still not entirely understood and is still a strongly researched area [1, 6]. A possible research goal is to discover and compare the energy consumption needed for balancing when standing still and during walking, running or hopping. The postural sway during standing still shows that certain energy input is required for the stabilization of the otherwise unstable upright standing position, similarly to the stabilization of an inverted pendulum via a feedback controller. Running, on the other hand, is a periodic motion for which the energy consumption can be divided into two parts: 1) the energy required for the recovery of dissipation and the energy loss due to dynamic reasons; and 2) the effort needed for the prevention of falling over. The energy required for the stabilization may actually be smaller in case of running than in case of standing still.

1.2. Models and results for ground-foot impact intensity

A mechanical model containing the foot and the shank was introduced in [11] for the investigation of the effect of the foot strike pattern. The foot-shank system falls vertically and the foot hits a fixed pin. The contact point position is characterized by the strike pattern s. A further developed but still two-segmented model was introduced in [9]. As an extension of the model in [11], a variable ankle angle and a horizontal velocity were introduced. Both [11] and [9] report that the effective mass and therefore the impact intensity is lower for forefoot-strike, when strike pattern is $s = 0.7 \dots 1$ than heel-strike, when $s = 0 \dots 0.2$.

Results in [14] showed that in addition to the strike pattern, the angle of the shank also strongly affects the properties of the ground-foot impact. The model in [14] involves the thigh and the total mass of the human body. The segments perform a rigid-body-like motion in the pre-impact phase with no relative motion of the body segments, which is not realistic.

A realistic pre-impact velocity condition can be obtained either from experiments or from a dynamic model that performs stable periodic running motion. In our previous work [3], we introduced such a dynamic model subjected to a torque control in order to perform further biomechanical analysis of human running performance. The advantage of this model over an experiment is that the control parameters can be tuned to optimize different cost functions, such as running speed, energy efficiency and impact intensity. Present paper reports new results about the detailed analysis of the model.

1.3. Existing segmented hopping leg models and related results

This subsection overviews a few models developed to perform stable periodic motion, like walking, hopping and running.

Many aspects of periodic motion of legged systems are detailed in [5], where several walking, running and hopping models are reviewed. The classical spring-loaded inverted pendulum (SLIP) model gives a fundamental background for hopping leg models. SLIP represents the body inertia as a point mass which bounces along on a single elastic massless leg. The supporting role of the leg in each stance phase is characterized by the SLIP.

Self-stable running-like locomotion is presented in [13] for a case where the inertia and dynamic effects of the segments are neglected and the body weight is modeled by a point mass in the hip. It is reported that the stable domain regarding landing angle and horizontal speed is larger than in case of SLIP model. The presence of massless segments leads to 1) smooth dynamics, i.e. there is no impulsive forces when the foot gets in contact with the ground; 2) the elimination of all inertial forces due to the inertia of the leg segments. These simplifications facilitates essential analytical and numerical results. Here, we extend this model in such way, that 1) the energy loss and impact forces are possible to be obtained, 2) the effects due to inertial forces are discovered. While the model in [13] is self-stable, in the extended model we use state feedback and control actions in order to achieve the stable hopping motion.

2. Dynamic model of the controlled hopping leg

The single-legged, planar mechanical model depicted in Fig. 1 is an extended combination of the ground-foot impact model in [14] and the self-stable hopping model in [13]. The new aspect is that a feedback controller is introduced to the model from [14], which was not actuated at all. In contrast with [13], self-stability without controller is not possible here, because the rigid body collision absorbs energy. Another extension is that the proposed control concept also involves a reaction wheel which is attached in the hip. The overall model consists of the equations of motion and the control algorithm similarly as in [3].

2.1. Mechanical structure

The three segments 1, 2 and 3 correspond to the foot, shank and thigh, respectively. Points A, B, C and D correspond to the tiptoe, the ankle, the knee and the hip, respectively. The reaction wheel plays the role of the upper body: the torque M_{D} that rotates the thigh has the reaction torque exerted on the wheel. The reaction wheel has mass m_{r} and moment of inertia J_{r}. The homogeneous, prismatic bars have masses m_i and lengths l_i, $i = 1 \ldots 3$. The centre of gravity is located at point G. The segments are interconnected by torsional springs with stiffnesses k_{B} and k_{C}. Actuating torques M_{B} and M_{C} assist the motion according to the control, which will be introduced below.

The model has a total of 6 DoFs in the flight phase: $\mathbf{q}^{\mathrm{f}} = [x_{\mathrm{A}}, z_{\mathrm{A}}, \theta_1, \theta_{12}, \theta_{23}, \theta_{\mathrm{r}}]$, where

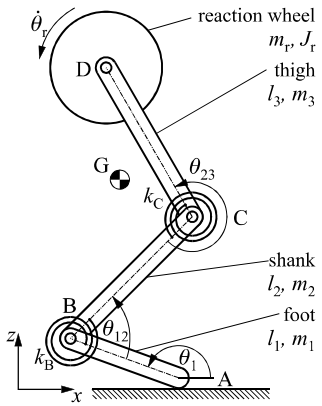

Figure 1. Segmented leg model

x_A and z_A are the Cartesian coordinates of the tiptoe. There are 4 DoFs in grounded phase: $\mathbf{q}^g = [\theta_1, \theta_{12}, \theta_{23}, \theta_r]$. In both phases, the equation of motion assumes the general form:

$$\mathbf{M}(\mathbf{q})\ddot{\mathbf{q}} + \mathbf{C}(\mathbf{q}, \dot{\mathbf{q}}) = \mathbf{Q}(\mathbf{q}, \dot{\mathbf{q}}) \,, \tag{1}$$

where $\mathbf{M} \in \mathbb{R}^{n \times n}$ is the mass matrix, $\mathbf{C} \in \mathbb{R}^n$ is the inertial force vector and $\mathbf{Q} \in \mathbb{R}^n$ general force contains the control torques. Here $\mathbf{q} = \mathbf{q}^f$ and $n = 6$ in flight-phase; while $\mathbf{q} = \mathbf{q}^g$ and $n = 4$ in ground-phase.

We assume that the ground-foot impact is completely inelastic, there is no rebound and the friction coefficient is high enough to prevent sliding of the foot. These assumptions allows us to constrain the tiptoe to the ground until the contact force is positive. See Section 3.1 for more details.

The non-linear spring characteristics, which is caused by the muscle-tendon dynamics, is not considered here in order to reduce the number of parameters. The torques exerted by the linear torsional springs of stiffness k_B and k_C are given by

$$k_B(\theta_{12} - \alpha_{12}) \qquad \text{and} \qquad k_C(\theta_{23} - \alpha_{23}) \,, \tag{2}$$

where α_{12} and α_{23} denotes the joint angle values that corresponds to unstretched springs.

The anatomical data adopted from [2] of a 24 years old average male with bodyweight of 73 kg and body height of 173.1 cm were considered (see Table 1).

2.2. Control

On the top of the spring torques, additional torques are exerted with respect to the control in equations (3) - (5) and (7) - (9). In our concept a control law is formulated that provides

Table 1. Inertial and geometric data of body segments

	mass	length/height	CoG mass moment of inertia
whole body	$m_\mathrm{b} = 73\,\mathrm{kg}$	$l_\mathrm{b} = 1.731\,\mathrm{m}$	-
trunk	$m_\mathrm{r} = 0.6028 m_\mathrm{b}$	-	$J_\mathrm{r} = 1.9778\,\mathrm{kgm}^2$
feet	$m_1 = 0.0274 m_\mathrm{b}$	$l_1 = 0.0885 l_\mathrm{b}$	$J_1 = 1/12 m_1 l_1^2$
shanks	$m_2 = 0.0866 m_\mathrm{b}$	$l_2 = 0.2470 l_\mathrm{b}$	$J_2 = 1/12 m_2 l_2^2$
thighs	$m_3 = 0.2832 m_\mathrm{b}$	$l_3 = 0.2320 l_\mathrm{b}$	$J_3 = 1/12 m_3 l_3^2$

periodic motion of the body. The motion of the segments is dictated by their dynamics, rather than having prescribed trajectories for the limb segments and a feedback control that forces the segment onto these prescribed trajectories. These two concepts are distinguished in [5]. Naturally, our control law needs the observation of the configuration of the segments and needs information about the actual flight/ground-phase of the leg.

2.2.1. Passive motion does not exist because of ground-foot impact

In general, the tiptoe touches the ground with non-zero velocity. This causes an impact and a certain kinetic energy loss, called *constrained motion space kinetic energy* (CMSKE) [9,14]. CMSKE is often used used as an energy efficiency indicator of passive walkers [4] because their energy loss is the foot impact only.

As a consequence, periodic hopping motion is not possible without some kind of energy input, which is provided by the muscles in humans and by motors in legged robots. An alternative possibility to avoid energy loss is to achieve zero-velocity collision, which means that the tiptoe velocity becomes zero at the instance of time when the foot touches down. However, impact-free motion does not guarantee periodicity, because the model can fall over, and using a controller is a more feasible approach.

2.2.2. Flight-phase

The vibrations of the leg segments are suppressed by M_B and M_C in the flight phase as (3) and (4) show. A proportional-derivative controller defined in (5) tries to keep the tiptoe (point A) at a specified horizontal position near to the centre of mass position x_G of the overall model in order to avoid falling over.

$$M_\mathrm{B}^\mathrm{f} = -D_\mathrm{B}\dot{\theta}_{12}\,, \tag{3}$$

$$M_\mathrm{C}^\mathrm{f} = -D_\mathrm{C}\dot{\theta}_{23}\,, \tag{4}$$

$$M_\mathrm{D}^\mathrm{f} = P(x_\mathrm{A} - (x_\mathrm{G} + x_\Delta)) + D(\dot{x}_\mathrm{A} - \dot{x}_\mathrm{G})\,. \tag{5}$$

Term x_Δ modifies the desired tiptoe position regarding the angular momentum Π_A calculated for point A. Furthermore, a constant K_v modifies the horizontal velocity:

$$x_\Delta = P_\Pi \, \Pi_\mathrm{A} - K_v \, . \tag{6}$$

2.2.3. Ground-phase

A certain part of the kinetic energy called CMSKE is absorbed in each stride because of the ground-foot impact. CMSKE is recovered by means of the control torques (7) and (8) exerted in the ankle and the knee. The goal is to keep the total mechanical energy E at the freely chosen desired energy level E_0. The mechanical power of these torques are positive only if the joints are in extension, so that $\dot{\theta}_{12}$ is positive and $\dot{\theta}_{23}$ is negative. Torque M^g_D in (9) prevents the continuous growth of the angular velocity $\dot{\theta}_\mathrm{r}$ of the reaction wheel.

$$M^\mathrm{g}_\mathrm{B} = P_E(E - E_0)\,\mathrm{sgn}(\dot{\theta}_{12}) \, , \tag{7}$$

$$M^\mathrm{g}_\mathrm{C} = P_E(E - E_0)\,\mathrm{sgn}(-\dot{\theta}_{23}) \, , \tag{8}$$

$$M^\mathrm{g}_\mathrm{D} = -P_\mathrm{r}\theta_\mathrm{r} - D_\mathrm{r}\dot{\theta}_\mathrm{r} \, . \tag{9}$$

2.2.4. Limitations

1) Depending on the configuration, bow and zigzag mode is possible, out of which only the latter is considered, because only this is possible for human leg. 2) There is no specific strategy for heel-strike yet. We consider hopping modes with ground-tiptoe contact only. 3) Since the segments are rigid, the behaviour of soft tissue is not possible yet. 4) As we mentioned earlier, the slip of the foot relative to the ground is not possible in this model. 5) The elastic-plastic behaviour of the ground is not considered.

3. Methods

Present work is based on numerical simulations of the hopping leg model, which was explained in Section 2. The most fundamental details are summarized in this Section.

3.1. Ground-foot impact intensity and energy loss

The foot touchdown is handled as an impulsive phenomenon, during which the velocity condition of the model goes under abrupt change. We assume that the ground-foot collision is instantaneous, which leads to infinitely large instantaneous forces over an infinitesimal time duration so that the net impulse due to the impact force is finite [9, 11]. Completely inelastic collision is also assumed, so that there is no rebound [9, 11, 14]. These assumptions lead us to consider the ground-foot contact as an instantly arising geometric constraint $\boldsymbol{\varphi}(\mathbf{q})$ as in [9, 14]. While velocity condition changes instantly, the configuration does not change.

Before foot touchdown, the system moves freely during flying phase. The new constraints $\boldsymbol{\varphi}(\mathbf{q}) = \mathbf{0}$ related to the ground contact arise at the time instant of the impact. The post-impact velocities are determined by the projection to the space of the admissible motion:

$$\dot{\mathbf{q}}^{+} = \mathbf{P}_a \dot{\mathbf{q}}^{-}, \tag{10}$$

where $\dot{\mathbf{q}}^{-} = \dot{\mathbf{q}}(t^{-})$ and $\dot{\mathbf{q}}^{+} = \dot{\mathbf{q}}(t^{+})$ are the pre- and post-impact generalized velocities respectively. $\mathbf{P}_{\mathrm{a}} = \mathbf{I} - \mathbf{P}_{\mathrm{c}}$ projects into the null-space of the constraint Jacobian $\boldsymbol{\Phi}_{\mathbf{q}} = \nabla_{\mathbf{q}} (\boldsymbol{\varphi})$, which is the subspace of the admissible motion. $\mathbf{P}_{\mathrm{c}} = \boldsymbol{\Phi}_{\mathbf{q}}^{\dagger} \boldsymbol{\Phi}_{\mathbf{q}}$ projects into the constrained subspace. The *generalised inverse* of the constraint Jacobian is calculated according to [10]:

$$\boldsymbol{\Phi}_{\mathbf{q}}^{\dagger} = \mathbf{M}^{-1} \boldsymbol{\Phi}_{\mathbf{q}}^{\mathrm{T}} (\boldsymbol{\Phi}_{\mathbf{q}} \mathbf{M}^{-1} \boldsymbol{\Phi}_{\mathbf{q}}^{\mathrm{T}})^{-1}. \tag{11}$$

The kinetic energy CMSKE related to the constrained motion vanishes when the foot touches the ground and can be calculated based on [8] as:

$$T_{\mathrm{c}} = \frac{1}{2} (\dot{\mathbf{q}}^{-})^{\mathrm{T}} \mathbf{P}_{\mathrm{c}}^{\mathrm{T}} \mathbf{M} \mathbf{P}_{\mathrm{c}} \dot{\mathbf{q}}^{-}. \tag{12}$$

Papers [9] and [8] showed that foot strike intensity can be characterised by the CMSKE which depends on the pre-impact configuration $\mathbf{q}^{-}$ and velocity $\dot{\mathbf{q}}^{-}$ and the *effective mass matrix* $\mathbf{M}_{\mathrm{e}} = \mathbf{P}_{\mathrm{c}}^{\mathrm{T}} \mathbf{M} \mathbf{P}_{\mathrm{c}}$. In this work the CMSKE is used for characterising the foot impact intensity: CMSKE is directly proportional to the impulse of the contact reaction force and also to the peak reaction force [8, 9].

3.2. Periodic paths and tuning of control parameters

Our goal is to find the control parameter set resulting stable periodic motion, while some cost function, like energy efficiency is minimized. We have 10 parameters in (3)-(9) collected in the vector $\mathbf{p} = [D_{\mathrm{B}}\,, D_{\mathrm{C}}\,, P\,, D\,, P_{\Pi}\,, K_v\,, P_E\,, E_0\,, P_{\mathrm{r}}\,, D_{\mathrm{r}}]$. Parameters $\mathbf{p}$ were tuned by trial-and-error method until periodic motion was possible to be found in [3] by means of *shooting method*.

For a given set of parameters $\mathbf{p}$, $\mathbf{x}_0^{*} = [\mathbf{q}_0^{*}\,, \dot{\mathbf{q}}_0^{*}]^{\mathrm{T}}$; $\mathbf{x}_0^{*} \in \mathbb{R}^{2n}$ is a periodic solution, if the system is in the same state at the beginning and at the end of the period, so that mapping $\mathbf{g}(\mathbf{x}_0, \mathbf{p})$ has a fix point or in other words $\mathbf{F}(\mathbf{x}_0^{*}, \mathbf{p}) = \mathbf{0}$, where

$$\mathbf{F}(\mathbf{x}_0, \mathbf{p}) = \mathbf{g}(\mathbf{x}_0, \mathbf{p}) - \mathbf{x}_0. \tag{13}$$

As Fig. 2 shows, the period starts at the beginning of the flight-phase and ends at the end of the ground-phase: event function $h_{\mathrm{g}\mapsto\mathrm{f}} = \lambda_{\mathrm{A}}$ crosses 0 in positive direction (λ_{A} is the vertical contact force magnitude). Transition from flight- to ground-phase occurs when

event function $h_{\mathrm{f}\mapsto\mathrm{g}} = z_{\mathrm{A}}$ crosses 0 in negative direction. Between flight- and ground phase a discontinuity mapping from $\mathbf{x}^-$ to $\mathbf{x}^+$ is realized by (10). Systems with such discontinuities are referred as *hybrid systems* in [12].

With a prosperous initial guess for $\mathbf{x}_0$, Newton-Raphson iteration provides the numerical approximation for $\mathbf{x}_0^*$ by finding the root of (13). The Jacobian $\mathbf{J} = \nabla_{\mathbf{x}_0}(\mathbf{F})$ is necessarily computed in the Newton-Raphson method, with which a possible approximation of the Jacobian $\mathbf{M} = \nabla_{\mathbf{x}_0}(\mathbf{g})$ of the mapping $\mathbf{g}$ can be computed as $\mathbf{M} = \mathbf{J} + \mathbf{I}$.

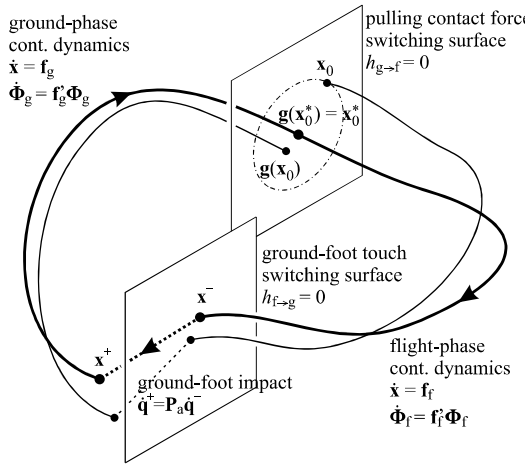

Figure 2. Schematic picture of a single period: flight-phase, ground-foot impact, ground-phase and ground foot detachment

The periodic orbit is stable, if a perturbed initial condition $\mathbf{x}_0$ is mapped ,,closer" to the periodic path. Due to the non-smoothness of our system, the accuracy of $\mathbf{M}$ is not sufficient for judging stability of the periodic path. Instead, the *flow Jacobian* is computed based on [12]. The following $2n + (2n)^2$ size ODE, which is referred as *first variational equation* in the literature, is solved during the continuous dynamics:

$$\dot{\mathbf{x}}(t) = \mathbf{f}(\mathbf{x}(t)); \quad \mathbf{x}(0) = \mathbf{x}_0\,, \tag{14}$$

$$\dot{\mathbf{\Phi}}(t) = \nabla_{\mathbf{x}}\left(\mathbf{f}(\mathbf{x}(t))\right)\mathbf{\Phi}(t); \quad \mathbf{\Phi}(0) = \mathbf{I}\,, \tag{15}$$

where $\mathbf{I}$ is $2n$ by $2n$ identity. Equations (14) and (15) can be applied with substitution $\mathbf{f} = \mathbf{f}_{\mathrm{f}}$ in flight-phase and $\mathbf{f} = \mathbf{f}_{\mathrm{g}}$ in ground-phase. Flow Jacobians $\mathbf{\Phi}_{\mathrm{f}}$ and $\mathbf{\Phi}_{\mathrm{g}}$ are obtained at the end of the flight- and ground-phase respectively. The Jacobian of the composite flow needs the Jacobian $\mathbf{S}$ of the discontinuity mapping, which is referred as *saltation matrix* in [12]. Finally the composite flow Jacobian, which can be reliably applied for determining stability of the periodic orbit, is obtained as $\tilde{\mathbf{\Phi}} = \mathbf{\Phi}_{\mathrm{g}}\mathbf{S}\mathbf{\Phi}_{\mathrm{f}}$.

The method described above makes possible to tune the parameters $\mathbf{p}$ in order to find the optimum for a certain cost function to be minimized. The cost function may be the norm of the largest eigenvalue of $\tilde{\mathbf{\Phi}}$, which characterizes stability. An other possible alternative for instance is to use T_c as cost function, which characterizes impact intensity. In order to find the minimum of the cost function, several numerical algorithms, like simplex method could be applied on the top of the above explained shooting method. The following sequence is repeated until the minimum of the cost function is found: the simplex method modifies $\mathbf{p}$, and the shooting method serves the solution $\mathbf{q}_0^*$ related to $\mathbf{p}$.

4. Results

Periodic paths was found for the control parameters that are collected in Table 2. Parameter E_0 was swept for $K_v = 0$ and 0.4 m fixed values. E_0 and K_v are responsible for the height and horizontal locomotion speed of the hopping motion respectively. Cases **A** and **B** are the smallest and largest possible E_0 values for $K_v = 0\,\mathrm{m}$ without loosing stability, while Cases **C** and **D** are the same for $K_v = 0.4\,\mathrm{m}$. The stiffness parameters were set to $k_\mathrm{B} = 1200\,\mathrm{Nm}$ and $k_\mathrm{C} = 1300\,\mathrm{Nm}$. The unstretchered angle of the springs are $\alpha_{12} = 80\,^\circ$ and $\alpha_{23} = 225\,^\circ$.

Table 2. Control parameters: E_0 and K_v are varied in the case examples, the rest are fixed

case	E_0 [J]	K_v [m]	D_B [Nms]	D_C [Nms]	P [N]	D [Ns]	P_Π $[(\mathrm{Ns})^{-1}]$	P_E [1]	P_r [Nm]	D_r [Nms]
A	752	0								
B	2970	0	15	20	950	50	0.01	0.2	4	15
C	1027	0.4								
D	3310	0.4								

4.1. Hopping motion with different speed and height

Hopping motion for four illustrative case examples are shown in Fig. 3. We found stable hopping motion from 0.018 to 2.141 m tiptoe elevation. The amplitude of the vertical centre of mass motion are 0.064 m in case **A**, 1.32 m in **B**, 0.071 m in **C** and 1.11 m in case **D**. The average locomotion v_x speed and the tiptoe elevation are plotted in the right panel of Fig. 3. A wide range of locomotion speed and hopping height is covered by tuning E_0 and K_v only, however we expect that the tuning of other control parameters provides larger stable domain.

4.2. Ground-foot impact intensity

The total kinetic energy T, the CMSKE (T_c) and the preserved part of the kinetic energy T_a are calculated for the ground-foot impact as Fig. 4 left panel shows. The normalized T_c and T_a on the right panel has a minimum value for the different values of the speed control

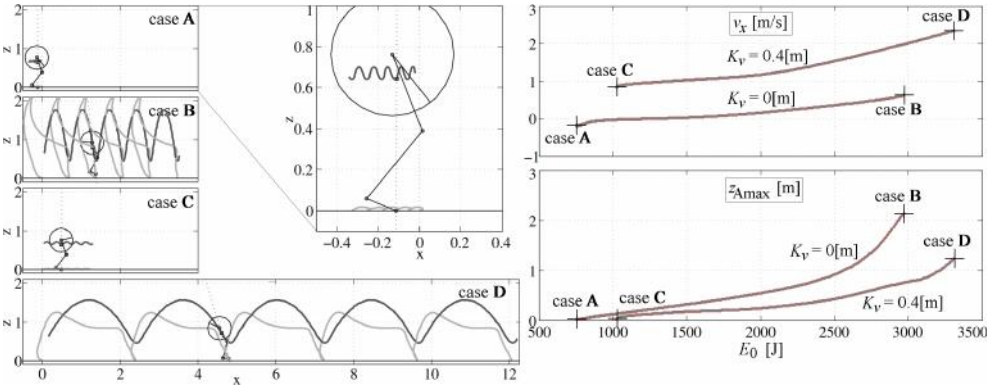

Figure 3. Results: the hopping motion with tiptoe and centre of mass path are illustrated in cases **A**, **B**, **C** and **D** in the left panel; the velocity v_x of the locomotion and the apex height z_{Amax} of the tiptoe path are plotted as the function of the desired energy level E_0.

parameter K_v. For $K_v = 0\,\mathrm{m}$ the optimal E_0 value is 821 J and 0.971 % of the kinetic energy is absorbed by the ground-foot impact. The optimum for $K_v = 0.4\,\mathrm{m}$ is $E_0 = 2230\,\mathrm{J}$ and the absorbed kinetic energy ratio is 2.09 %.

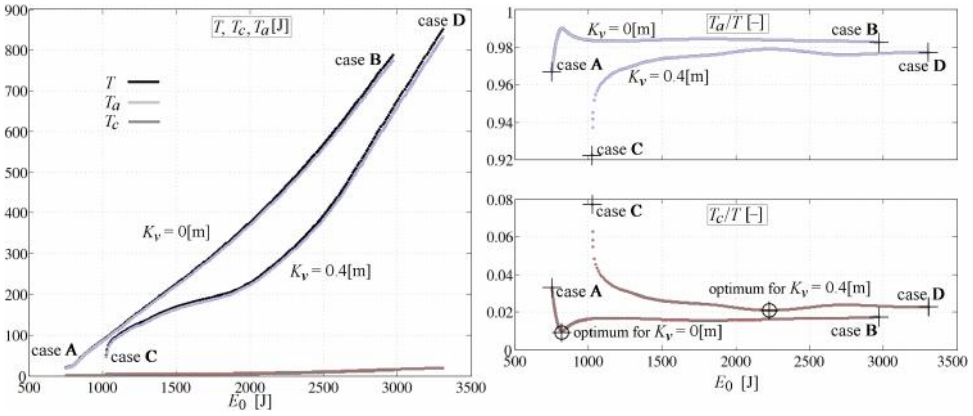

Figure 4. Results: the pre-impact kinetic energy T, the absorbed kinetic energy T_{c} related to the constrained subspace and the remaining kinetic energy T_{a} related to the admissible subspace are plotted in left panel; the normalized T_{c} and T_{a} are plotted in the right panel.

5. Conclusions and further steps

Stable periodic motion, i.e. running was achieved with the planar three-segmented leg model by means of control torques in the ankle and the knee joint and with a reaction wheel

placed at the hip. Wide range of locomotion velocity ($-0.2 \ldots 2.35\,\mathrm{m/s}$) and hopping motion height (tiptoe elevation: $0.018 \ldots 2.14\,\mathrm{m}$) were discovered, where the remaining fixed control parameters guaranteed stable operation. However, the currently fixed parameters will be tuned hereafter. The optimum of the hopping height was found, when the ground-foot impact intensity is the smallest and therefore the largest amount of kinetic energy is preserved.

We applied shooting method to obtain periodic orbits of the hybrid system. However, in future works, we plan to find and follow periodic orbits and their stability with advanced continuation methods. The model will be developed further in order to achieve more human-like motion; in particular, two legs and a more accurate model for the upper body can be considered. The model can also be used to investigate the effect of the terrain on the optimal motion, like inclination of the ground. Although some conclusion regarding human motion can be drawn from mathematically generated trajectories of the a model, a comparison with laboratory experiments with human subjects is also necessary. After refinement of the proposed mechanical model and the controller other performance measures of human running may become feasible.

References

[1] Chagdes, J., Rietdyk, S., Jeffrey, M., Howard, N., and Raman, A. Dynamic stability of a human standing on a balance board. journal of biomechanics. *Journal of Biomechanics 46*, 15 (2013), 2593–2602.

[2] de Leva, P. Adjustments to zatsiorsky-seluyanov's segment inertia parameters. *Journal of Biomechanics 29*, 9 (1996), 1223–1230.

[3] Fekete, L., Krauskopf, B., and Zelei, A. Three-segmented hopping leg for the analysis of human running locomotion. In *ENOC 2017 – 9th European Nonlinear Dynamics Conference* (Budapest, Hungary, 25-30, June 2017), pp. 1–2.

[4] Garcia., M., Chatterjee., A., Ruina, A., and Coleman, M. The simplest walking model: stability, complexity, and scaling. *Journal of Biomechanical Engineering 120* (1998), 281–288.

[5] Holmes, P., Full, R. J., Koditschek, D. E., and Guckenheimer, J. The dynamics of legged locomotion: Models, analyses, and challenges. *SIAM Rev. 48*, 2 (2006), 207–304.

[6] Insperger, T., and Milton, J. Sensory uncertainty and stick balancing at the fingertip. *Biological Cybernetics 108*, 1 (2016), 85–101. doi:10.1007/s00422-013-0582-2.

[7] Jungers, W. L. Barefoot running strikes back. *Nature, Biomechanics 463*, 7280 (2010), 433–434.

[8] Kövecses, J., and Font-Llagunes, J. M. An eigenvalue problem for the analysis of variable topology mechanical systems. *ASME Journal of Computational and Nonlinear Dynamics 4*, 3 (2009), 9 pages. doi:10.1115/1.3124784.

[9] Kövecses, J., and Kovács, L. L. Foot impact in different modes of running: mechanisms and energy transfer. *Procedia IUTAM 2* (Symposium on Human Body Dynamics, 2011), 101–108.

[10] Kövecses, J., Piedoboeuf, J.-C., and Lange, C. Dynamic modeling and simulation of constrained robotic systems. *IEEE/ASME Transactions on Mechatronics 2*, 2 (2003), 165–177.

[11] Lieberman, D. E., Venkadesan, M., Werbel, W. A., Daoud, A. I., D'Andrea, S., Davis, I. S., Mang'Eni, R. O., and Pitsiladis, Y. Foot strike patterns and collision forces in habitually barefoot versus shod runners. *Nature, Biomechanics 463*, 7280 (2010), 531–535.

[12] Piiroinen, P. T., and Dankowicz, H. J. Low-cost control of repetitive gait in passive bipedal walkers. *International Journal of Bifurcation and Chaos 15*, 6 (2005), 1959–1973.

[13] Rummel, J., and Seyfarth, A. Stable running with segmented legs. *Intl. Journal of Robotics Research 27*, 8 (2008), 919–934.

[14] Zelei, A., Bencsik, L., Kovács, L. L., and Stépán, G. Energy efficient walking and running - impact dynamics based on varying geometric constraints. In *12th Conference on Dynamical Systems Theory and Applications* (Lodz, Poland, 2-5, December 2013), pp. 259–270.

Ambrus Zelei, Ph.D. (Research Associate): Department of Applied Mechanics, Budapest University of Technology and Economics and MTA-BME Research Group on Dynamics of Machines and Vehicles, Muegyetem rkp. 3-5.,Budapest, 1111, Hungary (*zelei@mm.bme.hu*). The author gave a presentation of this paper during one of the conference sessions.

Bernd Krauskopf, Ph.D. (Professor): Department of Mathematics, University of Auckland, Private Bag 92019, Auckland 1142, New Zealand (*b.krauskopf@auckland.ac.nz*).

Tamás Insperger, Ph.D. (Associate Professor): Department of Applied Mechanics, Budapest University of Technology and Economics and MTA-BME Lendület Human Balancing Research Group, Muegyetem rkp. 3-5.,Budapest, 1111, Hungary (*insperger@mm.bme.hu*).